# THE NONLINEAR STABILITY OF A HEAVY RIGID PLATE SUPPORTED BY FLEXIBLE COLUMNS

W. I. Thacker†
Department of Computer Science, Winthrop University, Rock Hill,
South Carolina 29733, U.S.A.

C. Y. Wang
Departments of Mathematics and Mechanical Engineering, Michigan State University,
East Lansing, Michigan 48824, U.S.A.

and

L. T. Watson
Department of Computer Science, Virginia Polytechnic Institute and State University,
Blacksburg, Virginia 24061-0106, U.S.A.

**Abstract**—A heavy rigid platform is supported by thin elastic legs. The governing equations for large deformations are formulated and solved numerically by homotopy and quasi-Newton methods. Nonlinear phenomena such as nonuniqueness, catastrophe and hysteresis are found. A global critical load for nonlinear stability is introduced.

## 1. INTRODUCTION

Consider a structure composed of a heavy platform supported by four columns. Such a basic table-like configuration is fairly common in engineering construction. Our question is, if the legs are elastic, what is the maximum platform weight that can be supported?

The buckling of a rectangular frame has been considered before [e.g. Timoshenko and Gere (1961), McCormac and Elling (1988) and Gaylord and Gaylord (1990)]. It can be shown from linear analysis that the initial buckling of a supported rigid platform is due to side sway. The critical buckling load on each leg is $\pi^2 EI/L^2$, where $L$ is the length of the leg and $EI$ is its flexural rigidity.

Linear stability analysis, however, investigates the bifurcation or infinitestimal deviation from equilibrium. For large perturbations, such as those due to an earthquake, the maximum load that can be supported may be much smaller than that predicted by the linear theory.

## 2. FORMULATION

We illustrate this problem by the deformation of a two-dimensional table shown in Fig. 1(a). This is also equivalent to the four-legged table buckling along a symmetry axis. Let the height of the legs be $L$ and spaced $\beta L$ apart. The total load of the platform is acting at the center of gravity. We assume the platform to be rigid and the legs to be perfectly elastic.

Normalize all lengths by $L$ and all forces by $EI/L^2$. The general deformed shape and the forces $F_i$, $G$, moments $m_i$ ($i = 1, 2$) at the bases of leg 1 and leg 2 are shown in Fig. 1(b). Balancing the local moment on an elemental segment [Fig. 1(c)] we find

$$m_i + \mathrm{d}m_i + F_i\, \mathrm{d}s \sin \theta_i + (-1)^i G\, \mathrm{d}s \cos \theta_i = m_i. \tag{1}$$

Here $s$ is the arc length and $\theta_i$ is the local inclination angle with respect to the vertical. If the legs are thin enough, the Euler–Bernoulli (elastica) law
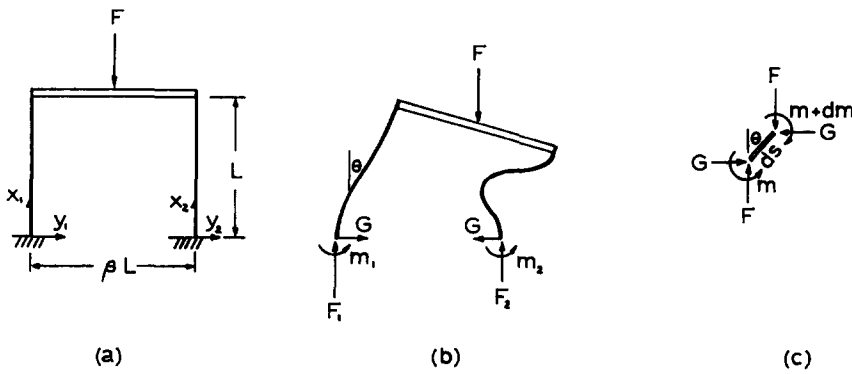
Fig. 1. The coordinate system, applied and internal forces.

$$m = \frac{\mathrm{d}\theta}{\mathrm{d}s} \tag{2}$$

is locally satisfied. Thus for equilibrium, the governing equations are

$$\frac{\mathrm{d}^2\theta_1}{\mathrm{d}s^2} + F_1 \sin \theta_1 - G \cos \theta_1 = 0, \tag{3}$$

$$\frac{\mathrm{d}^2\theta_2}{\mathrm{d}s^2} + F_2 \sin \theta_2 + G \cos \theta_2 = 0. \tag{4}$$

The kinematic conditions are

$$\frac{\mathrm{d}x_1}{\mathrm{d}s} = \cos \theta_1, \quad \frac{\mathrm{d}y_1}{\mathrm{d}s} = \sin \theta_1,$$

$$\frac{\mathrm{d}x_2}{\mathrm{d}s} = \cos \theta_2, \quad \frac{\mathrm{d}y_2}{\mathrm{d}s} = \sin \theta_2. \tag{5}$$

Given the total load $F$ and spacing $\beta$ there are 10 unknowns: $\theta_1$, $\mathrm{d}\theta_1/\mathrm{d}s$, $\theta_2$, $\mathrm{d}\theta_2/\mathrm{d}s$, $x_1$, $y_1$, $x_2$, $y_2$, $F_2$, $G$, $(F_1 = F - F_2)$. The 10 boundary conditions are, at the base

$$\theta_1(0) = \theta_2(0) = x_1(0) = x_2(0) = y_1(0) = 0, \tag{6}$$

$$y_2(0) = \beta, \tag{7}$$

and at the top,

$$\theta_1(1) = \theta_2(1), \tag{8}$$

$$\beta \cos \theta_1(1) = y_2(1) - y_1(1), \tag{9}$$

$$\beta \sin \theta_1(1) = x_1(1) - x_2(1). \tag{10}$$

The final condition is a global moment balance about the origin,

$$\frac{\mathrm{d}\theta_1}{\mathrm{d}s}(0) + \frac{\mathrm{d}\theta_2}{\mathrm{d}s}(0) + F_2\beta = F\left[\frac{y_1(1) + y_2(1)}{2}\right]. \tag{11}$$

Nontrivial solutions of eqns (3)–(11) are sought.

### 3. LIMITING CASES

As $\beta \to \infty$, the platform necessarily remains horizontal; we find

$$F_1 = F_2 = \frac{F}{2}, \quad G = 0. \tag{12}$$

The governing equation is then

$$\frac{d^2\theta_i}{ds^2} + \frac{F}{2}\sin\theta_i = 0 \tag{13}$$

with

$$\theta_i(0) = \theta_i(1) = 0. \tag{14}$$

Equations (13) and (14) can be linearized to give the bifurcation condition

$$\sin\left(\sqrt{F/2}\right) = 0 \quad \text{or} \quad F = 2n^2\pi^2. \tag{15}$$

We are concerned with the lowest buckling mode $n = 1$. Thus

$$F_c = 2\pi^2. \tag{16}$$

For nonlinear deformation, the solution to eqns (13) and (14) can be expressed in terms of elliptic functions $\mathscr{F}$. Multiply (13) by $\theta'$ and integrate. The constant of integration is determined by observing that the maximum angle $\gamma$ occurs at the symmetry point $s = 1/2$. Integrating again gives, in the notation of Abramowitz and Stegan (1972),

$$s = \int_0^{\theta(s)} \frac{dt}{\sqrt{F(\cos t - \cos \gamma)}} = \frac{2}{\sqrt{F(1 - \cos \gamma)}} \mathscr{F}\left(\frac{\theta}{2} \middle| \frac{2}{1 - \cos \gamma}\right), \tag{17}$$

where $\gamma = \theta(\tfrac{1}{2})$ is implicit in the solution.

The vertical displacement of the center of gravity is

$$\delta = 1 - \tfrac{1}{2}[x_1(1) + x_2(1)]. \tag{18}$$

The force–displacement relation of eqn (17) shows regular pitch-fork bifurcation at $2\pi^2$, then force continues to increase with displacement.

When $\beta = 0$ the two legs coalesce into one. The system is equivalent to a standing column with a tip load at the free end. The governing equation is still eqn (13) but with boundary conditions

$$\theta_i(0) = \frac{d\theta_i}{ds}(1) = 0. \tag{19}$$

The buckling force for the lowest mode is

$$F_c = \frac{\pi^2}{2}. \tag{20}$$

The solution and the force–displacement relations show similar behavior to the $\beta \to \infty$ case.

### 4. NUMERICAL METHODS

For finite nonzero $\beta$, the bifurcation, or linear stability, is still governed by the side-sway mode or $F_c = 2\pi^2$. Analytic post-buckling solutions, however, are almost impossible since

the boundary conditions cannot be applied to $\theta$, which is implicit in the elliptic functions. Thus a numerical solution is necessary.

The boundary value problem is defined by eqns (3)–(5) with boundary conditions (6)–(11). We have the unknowns $F$, $F_1$, $\beta$, $G$. $\theta'_1(0)$ and $\theta'_2(0)$. Since there are only four boundary conditions at 1, we can only solve for four variables; the rest must be given as parameters of the problem. We use $F$ and $\beta$ as the problem parameters. The unknowns are $\theta'_1(0)$, $\theta'_2(0)$, $G$ and $F_1$.

Let

$$
V = \begin{bmatrix} \theta'_1(0) \\ \theta'_2(0) \\ G \\ F_1 \end{bmatrix}, \tag{21}
$$

and let $\theta_1(\eta; V)$, $\theta_2(\eta; V)$, $x_1(\eta; V)$, $x_2(\eta; V)$, $y_1(\eta; V)$, $y_2(\eta; V)$ be the solution to the initial value problem given by eqns (3)–(7) with unknown values specified by $V$. The original two point boundary value problem is mathematically equivalent to solving the nonlinear system of equations

$$
\Psi(V) = \begin{bmatrix} \theta_1(1; V) - \theta_2(1; V) \\ \beta \cos(\theta_1(1; V)) - y_2(1; V) + y_1(1; V) \\ \beta \sin(\theta_1(1; V)) - x_1(1; V) + x_2(1; V) \\ \theta'_1(0) + \theta'_2(0) - \dfrac{F}{2}[y_1(1; V) + y_2(1; V)] + F_2\beta \end{bmatrix} = 0. \tag{22}
$$

The technique used is to guess at values for $V$ and solve the initial value problem equations (3)–(7) augmented with $V$. The software used for solving the initial value problem was the subroutine ODE from ODEPACK (Shampine and Gordon, 1975). Then $\Psi$ is evaluated and a new approximation to $V$ is computed. This technique is referred to as shooting (Keller, 1976).

This problem has multiple solutions for certain $F$ and $\beta$ values. The trivial solution $V = (0, 0, 0, F/2)^t$ is a solution for all $F$ and $\beta$. A quasi-Newton method, implemented in the subroutine HYBRJ from the MINPACK system (Moré *et al.*, 1980), was used to attempt to solve (22). However, starting points close enough to a nontrivial solution for the quasi-Newton method to converge to the solution could not be found. HYBRJ would either become stuck in a local minimum of $\Psi^t\Psi$ or converge to the trivial solution.

Next, a globally convergent homotopy based nonlinear system solver, subroutine FIXPDF from the HOMPACK (Watson *et al.*, 1987) suite of codes, was used. This method tracks the zero curve of

$$
\rho_a(V; \Lambda) = \Lambda\Psi(V) + (1 - \Lambda)(V - a), \tag{23}
$$

starting with $\Lambda = 0$. $\rho_a(V; 0) = 0$ when $V = a$, so a solution is known for $\rho_a(V; \Lambda) = 0$ when $\Lambda = 0$. From this starting point solutions of $\rho_a(V; \Lambda) = 0$ are tracked until $\Lambda = 1$. The HOMPACK codes track this curve allowing $\Lambda$ to decrease also. This is needed for many nonlinear systems and is not provided by most standard continuation methods.

The homotopy method did not have problems with local minima like the quasi-Newton methods. Whereas, FIXPDF always converged, it converged to the trivial solution. Hence, the problem was reformulated into an equivalent problem without a trivial solution. To accomplish this, the roles of $\theta'_1(0)$ and $F$ were reversed. So $\theta'_1(0)$ was a parameter (set to a nonzero value to give a nontrivial solution) and $F$ was placed in $V$. FIXPDF found a solution to this problem. Using this solution (a set of $F$, $\beta$, $\theta'_1(0)$, $\theta'_2(0)$, $F$, $F_1$), which is also a solution to eqns (3)–(11), as a starting point to HYBRJ, problems with slightly

different $F$ and $\beta$ were solved. Too large a step size could not be taken in $F$ or $\beta$ (especially $\beta$) or HYBRJ would not converge.

For a fixed $\beta$, we want to track the zero curve $\Gamma$ of

$$\Psi(V; F) \qquad (24)$$

as $F$ varies between some $F_0$ and $F_m$. This would be possible using HYBRJ if the solution $V = V(F)$ along the zero curve $\Gamma$. If $V$ is not a function of $F$ along $\Gamma$, HYBRJ cannot be used to advance the solution from a prior solution $(F_0, V_0)$ because $F$ can either increase or decrease along $\Gamma$. HOMPACK is designed to solve such problems, however, and the subroutine STEPS from HOMPACK can be used to trace $\Gamma$ between any two connected solutions $(F_0, V_0)$ and $(F_m, V_m)$.

The bifurcation diagrams (using vertical displacement of the midpoint $= 1 - (x_1(1) + x_2(1))/2$ as the independent variable) were produced using the zero curve results as input to the initial value solver ODE to get $x_1(1)$ and $x_2(1)$. The frames were plotted by reading $V$ into Mathematica (Wolfram, 1988) and having it solve the initial value problem for $x_1, y_1$ and $x_2, y_2$, then performing a parametric plot of these functions.

## 5. RESULTS AND DISCUSSION

Figure 2 shows the vertical displacement $\delta$ versus load $F$ for various normalized spacing $\beta$. The limiting case $\beta = 0$ is represented by the left dashed line starting from its critical load $F_c = \pi^2/2$. This is the load–displacement curve for a fixed-free column [see e.g. Timoshenko and Gere (1961)]. The limiting case for $\beta = \infty$ is governed by the right dashed curve, starting from the critical load $F_c = 2\pi^2$. This case is the same as the deformation of a fixed-fixed column. The displacements for both limiting cases rise monotonically with increased $F$ after buckling.

Of great interest are the curves for finite nonzero $\beta$. Incipient buckling is always through side sway from $F_c = 2\pi^2$. In general for small displacements, the curves tend to follow the $\beta = \infty$ limit while for larger displacements the curves seem to switch to the $\beta = 0$ limit. As a result, the curves are no longer monotonic and highly nonlinear.

Take, for example, the square frame $\beta = 1$ whose force–displacement curve is shown in Fig. 3. As the load is gradually increased, the frame remains square until $F_c = 2\pi^2$ is reached. Then the frame side sways through states $A$ and $B$. Any further increase in $F$ causes a catastrophic jump to state $G$, accompanied perhaps with violent oscillations to
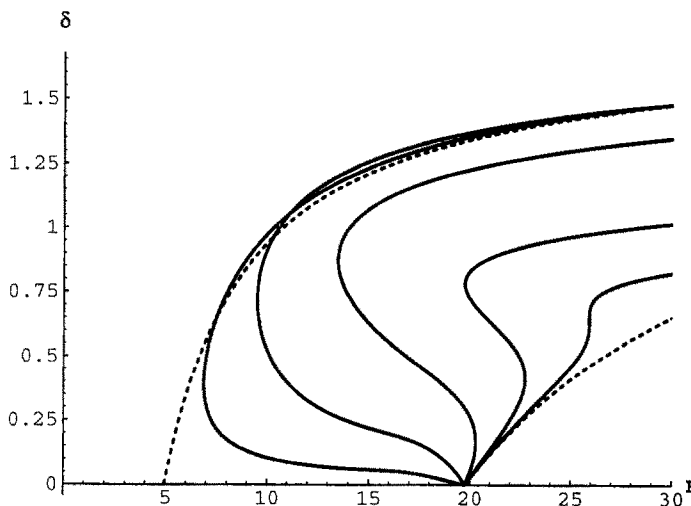


Fig. 2. Vertical displacement $\delta$ of center of gravity as a function of load $F$. Dashed lines are limiting cases. $\beta = 0, 0.125, 0.25, 0.5, 1.1095, 2.516, \infty$ (left to right).
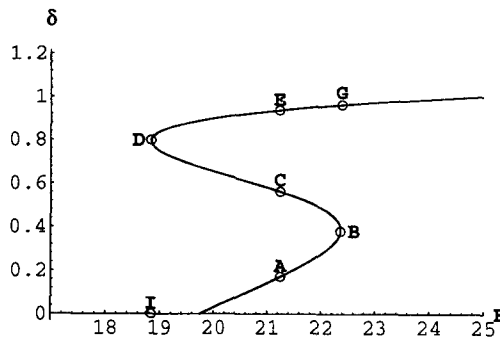
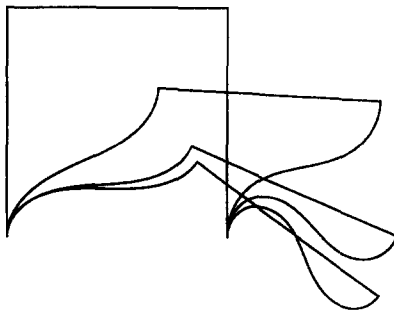Fig. 3. Vertical displacement versus load for $\beta = 1$ case. Note hysteresis loop IBGDI.



Fig. 4. Deformed configurations in the loop corresponding to states I, B, D, G (top to bottom), shown in Fig. 3.

dissipate excess energy. Now if $F$ is decreased from state $G$, the frame follows states $E$, $D$, then if $F$ decreases further, there is a sudden snap-back into the square frame at state $I$. Some configurations for the hysteresis loop are shown in Fig. 4. Notice the range of multiple solutions for $18.84 < F < 22.37$. The three solutions for the same $F = 21.2$ are shown in Fig. 5. Since the segment $BCD$ in Fig. 3 has negative slope (increased displacement causes negative work) state $C$ can never be realized in practice. Multiple solutions occur for the range $0 < \beta < 2.516$.

The usual definition of a statically stable structure is one which returns to its undeformed state after small perturbations are removed. Thus a vertical elastic fixed-free column is stable if $F < F_c = \pi^2/2$ and for our frames this stability criteria is $F < F_c = 2\pi^2$. However, the bifurcation curves of our frames are usually not monotonic as that of an Euler column. Figure 3 shows the frame may not be stable even for $F < F_c$ in the range $18.8 < F < 2\pi^2$, i.e. a large enough perturbation (in $\delta$) may force the frame to settle on a state on the DE segment and does not return to the undeformed state.
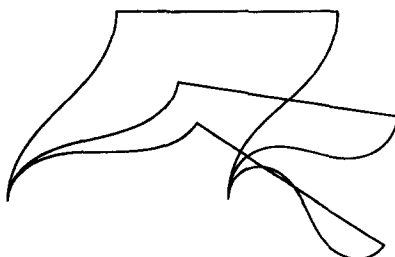


Fig. 5. Multiple solutions for the same $F = 21.2$ ($A$, $C$, $E$, in Fig. 3, top to bottom) $\beta = 1$.
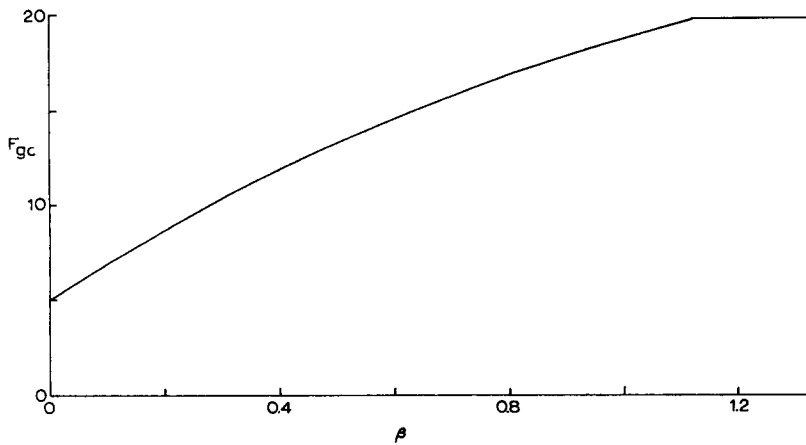
Fig. 6. Global critical load $F_{gc}$ as a function of $\beta$.

Let us define the *global critical load* under which the structure would return to its undeformed state however large the disturbances. For example if $F < F_{gc} = 18.8$, our square frame is globally stable. Such an index is extremely useful for flexible structures prone to large disturbances, e.g. earthquakes. Figure 6 shows the computed $F_{gc}$ as a function of $\beta$. When $\beta = 0$, $F_{gc}$ is $\pi^2/2$ and rises with $\beta$ until $\beta = 1.1095$, then it remains constant at $2\pi^2$ when $\beta$ is further increased. We see that for small $\beta$, $F_{gc}$ is significantly lower than the critical load of $2\pi^2$ for side sway under small disturbances.

In our large deformation analyses, we have allowed legs and platform and "ground" to cross each other as in state $G$ of Fig. 4. These situations are physically possible. Restraints on deformation only increase stability and $F_{gc}$ would be a safer upper bound.

## REFERENCES

Abramowitz, M. and Stegan, I. A. (1972). *Handbook of Mathematical Functions*. Dover, New York.

Frisch-Fay, R. (1962). *Flexible Bars*. Butterworths, Washington, DC.

Gaylord, E. H. and Gaylord, C. N. (Eds) (1990). *Structural Engineering Handbook* (3rd Edn). McGraw-Hill, New York.

Keller, H. B. (1976). *Numerical Solution of Two-Point Boundary Value Problems*. Society for Industrial and Applied Mathematics, Philadelphia.

McCormac, J. and Elling, R. E. (1988). *Structural Analysis*. Harper and Row, New York.

Moré, J. J., Garbow, B. S. and Hillstrom, K. E. (1980). *User Guide for MINPACK-1, ANL-80-74*. Argonne National Laboratory, Argonne.

Shampine, L. F. and Gordon, M. K. (1975). *Computer Solution of Ordinary Differential Equations*. W. H. Freeman, San Francisco.

Timoshenko, S. P. and Gere, J. M. (1961). *Theory of Elastic Stability*. McGraw-Hill, New York.

Watson, L. T., Billups, S. C. and Morgan, A. P. (1987). HOMPACK: a suite of codes for globally convergent homotopy algorithms. *ACM Trans. Math. Software* 3, 281–310.

Wolfram, S. (1988). *Mathematica, A System for Doing Mathematics by Computer*. Addison-Wesley, Redwood City, CA.